Pergamon

Int. J. Solids Structures Vol. 33, No. 30, pp. 4605–4624, 1996

0020–7683/96 $15.00 + .00

0020–7683(95)00280–X

DYNAMIC ANALYSIS OF TWO-DIMENSIONAL FRICTIONAL CONTACT BY LINEAR COMPLEMENTARITY PROBLEM FORMULATION

JUN O KIM and BYUNG MAN KWAK†
Department of Mechanical Engineering, Korea Advanced Institute of Science and Technology, 373-1, Kusong-dong, Yusong-gu, Taejon 305-701, Korea

(*Received* 16 *October* 1994; *in revised form* 9 *November* 1995)

Abstract—Two-dimensional dynamic contact is formulated as a linear complementarity problem using contact compatibility conditions and the Coulomb friction law. For the time integration of dynamic response, displacements are approximated as second-order polynomials and a new scheme of considering velocity discontinuities is presented. The efficiency of the method is shown with three numerical examples. Copyright © 1996 Elsevier Science Ltd

INTRODUCTION

Although shock or impact analysis is very important, local phenomena are often not properly treated due to lack of analysis methods. A precise formulation of the contact in dynamic simulation is not yet available. Current approximate methods are mainly based on the finite element method (FEM) and can be classified into two groups according to the treatment of contact and friction conditions. The first group assumes the contact region and contact status (stick, slip, or separation) first and then solves the problem and checks if the assumption is correct (Hughes *et al.*, 1976; Ko and Kwak, 1992a,b). They iteratively solve the problem by trial-and-error, thus requiring much computational effort. The second group transforms the original problem into a mathematical programming problem and solves it by quadratic programming techniques (Talaslidis and Panagiotopoulos, 1982; Chen and Tsai, 1986; Huh and Kwak, 1991). This approach can reduce the computational effort compared to the first group; however, the friction condition is not well treated and remains a challenge.

In this paper a new method for dynamic analysis of two-dimensional frictional contact problems is presented. From Hamilton's law the discretized equation of motion is derived using FEM. From a contact condition and the Coulomb friction law the problem is transformed into a set of linear complementarity relations for a time step analysis. Also a new way of considering the velocity discontinuities during impact is proposed. Three examples are used to show the efficiency of the method.

GOVERNING EQUATIONS

As shown in Fig. 1, consider two elastic bodies Ω^1 and Ω^2 which are brought into dynamic contact. Each boundary of the two bodies is composed of three disjoint parts Γ_u where displacement is prescribed, Γ_f where traction boundary conditions are given, and Γ_c which is the so-called potential contact region, taken as sufficiently large to include the real contact surface. The governing equations are derived extending those of a static problem, formulated in complementarity relations (Kwak, 1991; Kwak and Lee, 1988). They are described in the following section with minimum duplication of previous results from Kwak *et al.*

† To whom correspondence should be addressed.

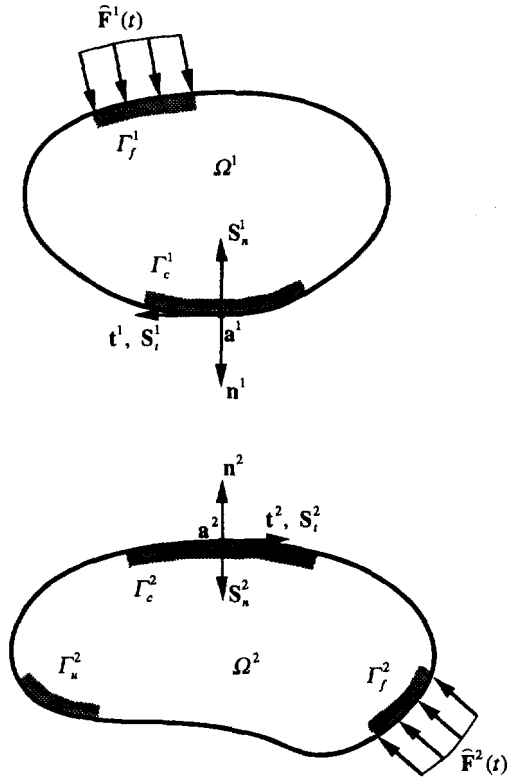

Fig. 1. Two bodies in contact.

(1) *Internal equilibrium of each body*

$$\sigma_{ij,j} + b_i - \rho \ddot{u}_i = 0 \quad \text{in } \Omega \equiv \Omega^1 \cup \Omega^2, \tag{1}$$

where σ_{ij}, b_i and u_i denote the Cauchy stress tensor, body force and displacement, respectively, and ρ denotes the density. The notation $(\ )_{,j}$ denotes differentiation with respect to the coordinate x_j and $(\dot{\ })$ denotes a time differentiation. An index notation with the usual summation convention is used throughout the paper.

(2) *Strain–displacement relation*

$$\varepsilon_{ij} = \tfrac{1}{2}(u_{i,j} + u_{j,i}) \quad \text{in } \Omega, \tag{2}$$

where ε_{ij} denotes the Cauchy strain.

(3) *Stress–strain relation*

$$\sigma_{ij} = C_{ijkl}\varepsilon_{kl} \quad \text{in } \Omega, \tag{3}$$

where C_{ijkl} denotes the matrix of elastic constitutive coefficients.

(4) *Initial conditions*

$$u_i = u_{0i} \quad \text{in } \Omega, \tag{4}$$

$$\dot{u}_i = \dot{u}_{0i} \quad \text{in } \Omega, \tag{5}$$

where u_{0i} and $\dot{u}_{0i}$ denote the prescribed initial displacement and velocity at time $t = t_0$, respectively, t_0 being the initial time.

(5) *Boundary conditions*

Displacement boundary conditions are

$$u_i = \hat{u}_i \quad \text{on } \Gamma_u, \tag{6}$$

where $\hat{u}_i$ is the given displacement. The traction boundary conditions are

$$\sigma_{ij} n_j = \hat{F}_i \quad \text{on } \Gamma_f, \tag{7}$$

where $\hat{F}_i$ denotes the given traction and n_j is the outward unit normal vector on Γ_f.

(6) *Compatibility condition*

The geometric compatibility condition has been generally described by Kwak (1991). Let D_n denote the contact gap between the two bodies. Then the impenetration condition is stated as

$$D_n \geqslant 0 \quad \text{on } \Gamma_c. \tag{8}$$

Since bonding between the bodies is not considered, the normal traction between two bodies must be compressive or zero, i.e.,

$$S_n \equiv -\sigma_{ij} n_i n_j \geqslant 0 \quad \text{on } \Gamma_c, \tag{9}$$

where S_n denotes the compressive normal traction or pressure. Since either the contact gap or the corresponding contact normal traction must be equal to zero for all pairs of opposing points, the following condition should be satisfied:

$$D_n \cdot S_n = 0 \quad \text{on } \Gamma_c. \tag{10}$$

(7) *Coulomb friction condition*

The normal traction and tangential traction should satisfy the Coulomb friction law:

$$-\mu S_n \leqslant S_t \leqslant \mu S_n \quad \text{on } \Gamma_c, \tag{11}$$

where $S_t \equiv \sigma_{ij} n_j t_i$ denotes the tangential traction, t_i the tangential unit vector, and μ the friction coefficient.

(8) *Impact condition*

When two bodies are brought into contact, the relative velocity normal to the contact surface should vanish. Also, when a pair of opposing material particles are in sticking status, their relative velocity tangential to the contact surface should be zero. These can be described as follows:

$$\dot{D}_n = 0 \quad \text{for } S_n > 0 \quad \text{on } \Gamma_c, \tag{12}$$

$$\dot{D}_t = 0 \quad \text{for stick state on } \Gamma_c, \tag{13}$$

where $\dot{D}_n$ and $\dot{D}_t$ denote the normal and tangential components of the relative velocity of the pair of opposing points.

FINITE ELEMENT FORMULATION

Hamilton's law (Bailey, 1975, 1980) can be adopted for frictional dynamic contact problems over the time interval $[t_n, t_n + \Delta t]$ for a material body Ω as follows:

$$\int_{t_n}^{t_n+\Delta t} \delta(T-V)\,\mathrm{d}t+\int_{t_n}^{t_n+\Delta t} \delta W_{nc}\,\mathrm{d}t-\int_{\Omega} \rho\dot{u}_i\,\delta u_i\,\mathrm{d}\Omega\Big|_{t_n}^{t_n+\Delta t}=0 \tag{14}$$

subject to eqns (4)–(6) and

$$D_n \cdot S_n = 0, \quad D_n \geqslant 0, \quad S_n \geqslant 0, \tag{15}$$

$$-\mu S_n \leqslant S_t \leqslant \mu S_n, \tag{16}$$

$$\dot{D}_n = 0 \quad \text{for } S_n > 0, \tag{17}$$

$$\dot{D}_t = 0 \quad \text{for stick state}, \tag{18}$$

where

$$T=\int_{\Omega} \tfrac{1}{2}\rho\dot{u}_i\dot{u}_i\,\mathrm{d}\Omega,$$

$$V=\int_{\Omega} \tfrac{1}{2}\sigma_{ij}\,\varepsilon_{ij}\mathrm{d}\Omega,$$

$$\delta W_{nc}=\int_{\Omega} b_i\,\delta u_i\,\mathrm{d}\Omega+\int_{\Gamma_f} \hat{F}_i\,\delta u_i\,\mathrm{d}\Gamma_f+\int_{\Gamma_c} (S_t t_i - S_n n_i)\,\delta u_i\,\mathrm{d}\Gamma_c \tag{19}$$

and they represent kinetic energy, elastic energy and virtual work done by external forces and contact forces, respectively. The variables u_i, S_n, and S_t are unknowns to be solved and denote the displacement of the bodies, normal and tangential tractions, respectively, while D_n and D_t can be represented in terms of u_i. It can be easily shown that taking a variation of eqn (14) together with constraint eqns (15)–(18) results in the governing equations previously described.

Following the usual finite element discretization procedure (Bathe, 1982), the displacement $\mathbf{u}$ of the bodies is approximated by using a nodal displacement vector $\mathbf{U}$ as

$$\mathbf{u}(\mathbf{x}, t) = \mathbf{H}(\mathbf{x})\mathbf{U}(t), \tag{20}$$

where $\mathbf{H}(\mathbf{x})$ denotes the shape function. Then the kinetic energy, elastic energy and the virtual work done by the external forces are arranged in matrix form as

$$T=\tfrac{1}{2}\dot{\mathbf{U}}^{\mathrm{T}}\mathbf{M}\dot{\mathbf{U}},$$

$$V=\tfrac{1}{2}\mathbf{U}^{\mathrm{T}}\mathbf{K}\mathbf{U},$$

$$\int_{\Omega} b_i\,\delta u_i\,\mathrm{d}\Omega+\int_{\Gamma_f} \hat{F}_i\,\delta u_i\,\mathrm{d}\Gamma_f=\delta\mathbf{U}^{\mathrm{T}}\mathbf{F}, \tag{21}$$

where

$$\mathbf{M}=\int_{\Omega} \rho\mathbf{H}^{\mathrm{T}}\mathbf{H}\mathrm{d}\Omega, \quad \mathbf{K}=\int_{\Omega} \mathbf{B}^{\mathrm{T}}C\mathbf{B}\mathrm{d}\Omega \quad \text{and} \quad \mathbf{F}=\int_{\Omega} \mathbf{H}^{\mathrm{T}}\mathbf{b}\mathrm{d}\Omega+\int_{\Gamma_f} \mathbf{H}^{\mathrm{T}}\hat{\mathbf{F}}\mathrm{d}\Gamma_f \tag{22}$$

denote mass matrix, stiffness matrix and load vector due to external forces, respectively. The matrix $\mathbf{B}$ is a strain–displacement matrix and $\mathbf{C}$ a stress–strain matrix.

Consider a contact pair comprised of two points $\mathbf{a}^1$ and $\mathbf{a}^2$ as shown in Fig. 1 and let $\tau = t - t_n \in [0, \Delta t]$. Then the contact gap at time $t_n + \tau$ can be linearized as

$$D_n = n_i^2(u_i^1 - u_i^2) - n_i^2(\bar{u}_i^1 - \bar{u}_i^2) + D_{n0} \tag{23}$$

where $\bar{u}_i^k$ denotes the displacement of body k at time t_n and $D_{n0} \equiv n_i^2(a_i^1 - a_i^2)$ the initial gap at $t = t_n$. The tangential slip during $[t_n, t_n + \tau]$ can be similarly represented as

$$D_t = t_i^2(u_i^1 - u_i^2) - t_i^2(\bar{u}_i^1 - \bar{u}_i^2). \tag{24}$$

For all contact pairs on Γ_c of the discretized model, the vectors of the contact gap and the relative slip can be written in array forms as

$$\mathbf{D}_n = \mathbf{D}_{nu}(\mathbf{U} - \bar{U}) + \mathbf{D}_{n0}, \tag{25}$$

$$\mathbf{D}_t = \mathbf{D}_{tu}(\mathbf{U} - \bar{U}), \tag{26}$$

where D_{n0} and $\bar{U}$ denote the contact gap and the displacement vector at time $t = t_n$, respectively. The matrices $\mathbf{D}_{nu}$ and $\mathbf{D}_{tu}$ are calculated at $t = t_n$, and consist of zeros and direction cosines of the normal vector at the contact surface coming from eqns (23) and (24). Now the virtual work done by the contact forces is expressed as follows:

$$\int_{\Gamma_c} (S_t t_i - S_n n_i)\, \delta u_i \, \mathrm{d}\Gamma_c = \mathbf{P}_n^{\mathrm{T}}\, \delta \mathbf{D}_n + \mathbf{P}_t^{\mathrm{T}}\, \delta \mathbf{D}_t = \delta \mathbf{U}^{\mathrm{T}}(\mathbf{D}_{nu}^{\mathrm{T}}\, \mathbf{P}_n + \mathbf{D}_{tu}^{\mathrm{T}}\, \mathbf{P}_t), \tag{27}$$

where $\mathbf{P}_n$ and $\mathbf{P}_t$ denote vectors of the normal and tangential nodal forces at the potential contact surfaces.

The last term in eqn (14) becomes

$$\int_{\Omega} \rho \dot{u}_i\, \delta u_i \, \mathrm{d}\Omega = \delta \mathbf{U}^{\mathrm{T}} \mathbf{M} \dot{\mathbf{U}}. \tag{28}$$

Contact condition (15) and friction condition (16) can be represented in discretized form:

$$\mathbf{D}_n^{\mathrm{T}}\, \mathbf{P}_n = 0, \quad \mathbf{D}_n \geqslant 0, \quad \mathbf{P}_n \geqslant 0, \tag{29}$$

$$-\mu \mathbf{P}_n \leqslant \mathbf{P}_t \leqslant \mu \mathbf{P}_n. \tag{30}$$

It is noted that eqn (29) is equivalent to $D_{nj} P_{nj} = 0$, $D_{nj} \geqslant 0$, $P_{nj} \geqslant 0$ for each j (no summation on j) and eqn (30) means $-\mu P_{nj} \leqslant P_{tj} \leqslant \mu P_{nj}$ for each j.

Now plugging eqns (21), (27), and (28) into eqn (14), the equation of motion for the discretized domain can be obtained as

$$\mathbf{M}\ddot{\mathbf{U}} + \mathbf{K}\mathbf{U} = \mathbf{F} + \mathbf{D}_{nu}^{\mathrm{T}}\, \mathbf{P}_n + \mathbf{D}_{tu}^{\mathrm{T}}\, \mathbf{P}_t. \tag{31}$$

Let us assume that impact occurs at $\tau = \tau_i \in [0, \Delta t]$. Integrating eqn (31) over $[\tau_i - 0, \tau_i + 0]$, the discontinuities of velocity due to impact can be accounted for as

$$\dot{\mathbf{U}}(\tau_i + 0) = \dot{\mathbf{U}}(\tau_i - 0) + \mathbf{M}^{-1}\mathbf{D}_{nu}^{\mathrm{T}}\, \Phi + \mathbf{M}^{-1}\mathbf{D}_{tu}^{\mathrm{T}}\, \Psi, \tag{32}$$

where

$$\Phi = \int_{\tau_i - 0}^{\tau_i + 0} \mathbf{P}_n \, \mathrm{d}\tau \quad \text{and} \quad \Psi = \int_{\tau_i - 0}^{\tau_i + 0} \mathbf{P}_t \, \mathrm{d}\tau. \tag{33}$$

In solving the discretized equation of motion, the direct time integration by Zienkiewicz

et al. (1984) is adopted. The nodal displacement vector $\mathbf{U}(t)$ over $\Delta(t)$ is approximated with second-order polynomials as

$$\mathbf{U} = N_i(t)\mathbf{U}^i = N_1\mathbf{U}^1 + N_2\mathbf{U}^2 + N_3\mathbf{U}^3, \tag{34}$$

where $\mathbf{U}^1$, $\mathbf{U}^2$ and $\mathbf{U}^3$ denote the values $\mathbf{U}(t)$ at time $\tau = 0$, $\Delta t/2$ and Δt, respectively, and N_i the shape function in time domain and are taken as

$$N_1 = \tfrac{1}{2}\eta(\eta-1), N_2 = 1-\eta^2 \quad \text{and} \quad N_3 = \tfrac{1}{2}\eta(\eta+1), \tag{35}$$

where $\eta = (2\tau/\Delta t) - 1$ and $\eta \in [-1, 1]$. Then the nodal velocity vector $\dot{\mathbf{U}}$ and acceleration vector $\ddot{\mathbf{U}}$ are approximated as

$$\dot{\mathbf{U}} = \dot{N}_i(\tau)\mathbf{U}^i = \dot{N}_1\mathbf{U}^1 + \dot{N}_2\mathbf{U}^2 + \dot{N}_3\mathbf{U}^3, \tag{36}$$

$$\ddot{\mathbf{U}} = \ddot{N}_i(\tau)\mathbf{U}^i = \ddot{N}_1\mathbf{U}^1 + \ddot{N}_2\mathbf{U}^2 + \ddot{N}_3\mathbf{U}^3. \tag{37}$$

Applying the initial condition $\dot{\mathbf{U}}(\tau = 0) = 2/\Delta t\, \dot{\mathbf{U}}(\eta = -1) = \dot{\mathbf{U}}^1$ to eqn (36), the following relation is obtained:

$$\mathbf{U}^2 = \tfrac{3}{4}\mathbf{U}^1 + \tfrac{1}{4}\mathbf{U}^3 + \tfrac{1}{4}(\Delta t)\dot{\mathbf{U}}^1. \tag{38}$$

If we assume a velocity jump at $\tau = 0$ as in eqn (32), then

$$\mathbf{U}^2 = \tfrac{3}{4}\mathbf{U}^1 + \tfrac{1}{4}\mathbf{U}^3 + \tfrac{1}{4}(\Delta t)[\dot{\mathbf{U}}^1 + \mathbf{M}^{-1}\mathbf{D}_{nu}^{\mathrm{T}}\Phi^0 + \mathbf{M}^{-1}\mathbf{D}_{tu}^{\mathrm{T}}\Psi^0], \tag{39}$$

where two vectors Φ^0 and Ψ^0 denote the values of Φ and Ψ at $\tau = 0$, respectively.

Applying the weighted residual method to eqn (31) we can get a weak form as

$$\int_0^{\Delta t} W(\tau)(\mathbf{M}\ddot{\mathbf{U}} + \mathbf{K}\mathbf{U} - \mathbf{F} - \mathbf{D}_{nu}^{\mathrm{T}}\mathbf{P}_n - \mathbf{D}_{tu}^{\mathrm{T}}\mathbf{P}_t)\,\mathrm{d}\tau = \mathbf{0}, \tag{40}$$

where $W(\tau)$ is a weighting function. Substituting eqns (34), (37) and (39) into eqn (40) and dividing by $\int_0^{\Delta t} W\,\mathrm{d}t$, one obtains the displacement $\mathbf{U}^3$ at $\tau = \Delta t$ as

$$\mathbf{U}^3 = \mathbf{M}^{*-1}[(\mathbf{M}^* - \mathbf{K})\mathbf{U}^1 + \mathbf{F}^* + \mathbf{D}_{nu}^{\mathrm{T}}\mathbf{P}_n^* + \mathbf{D}_{tu}^{\mathrm{T}}\mathbf{P}_t^* + (\Delta t)(\mathbf{M}^* - \gamma\mathbf{K})(\dot{\mathbf{U}}^1 + \mathbf{M}^{-1}\mathbf{D}_{nu}^{\mathrm{T}}\Phi^0 + \mathbf{M}^{-1}\mathbf{D}_{tu}^{\mathrm{T}}\Psi^0)], \tag{41}$$

where

$$\mathbf{M}^* = \frac{2}{(\Delta t)^2}\mathbf{M} + 2\beta\mathbf{K},$$

$$\beta = \frac{\int_{-1}^{1} W(\eta+1)^2\,\mathrm{d}\eta}{8\int_{-1}^{1} W\,\mathrm{d}\eta} = \frac{\int_0^{\Delta t} W\tau^2\,\mathrm{d}\tau}{2\Delta t^2\int_0^{\Delta t} W\,\mathrm{d}\tau},$$

$$\gamma = \frac{\int_{-1}^{1} W(\eta+1)\,d\eta}{2\int_{-1}^{1} W\,d\eta} = \frac{\int_{0}^{\Delta t} W\tau\,d\tau}{\Delta t\int_{0}^{\Delta t} W\,d\tau},$$

$$\mathbf{F}^* = \int_{-1}^{1} W\mathbf{F}\,d\eta \Big/ \int_{-1}^{1} W\,d\eta,$$

$$\mathbf{P}_n^* = \int_{-1}^{1} W\mathbf{P}_n\,d\eta \Big/ \int_{-1}^{1} W\,d\eta,$$

$$\mathbf{P}_t^* = \int_{-1}^{1} W\mathbf{P}_t\,d\eta \Big/ \int_{-1}^{1} W\,d\eta. \tag{42}$$

The velocity at $\tau = \Delta t$ is derived using eqn (36) as

$$\dot{\mathbf{U}}^3 = \frac{2}{\Delta t}(\mathbf{U}^3 - \mathbf{U}^1) - \dot{\mathbf{U}}^1 - \mathbf{M}^{-1}\mathbf{D}_{nu}^{\mathrm{T}}\Phi^0 - \mathbf{M}^{-1}\mathbf{D}_{tu}^{\mathrm{T}}\Psi^0. \tag{43}$$

The recurrence formula given by eqns (41) and (43) are implicit and self-starting. The variables $\mathbf{F}^*$, $\mathbf{P}_n^*$ and $\mathbf{P}_t^*$ denote weighted time averages over the time interval Δt. When $W(\tau) = \delta(\tau) + \delta(\tau - \Delta t)$, where $\delta(\bullet)$ denotes the Dirac delta function, one obtains $\gamma = 0.5$ and $\beta = 0.25$, typically used in practice. The input $\mathbf{F}^*$ may be taken as

$$\mathbf{F}^* = (1-\gamma)\mathbf{F}^1 + \gamma\mathbf{F}^3, \tag{44}$$

where $\mathbf{F}^1$ and $\mathbf{F}^3$ denote the values of $\mathbf{F}$ at $\tau = 0$ and $\tau = \Delta t$. Otherwise $\mathbf{F}^*$ can be directly input instead of specifying $W(\tau)$ and calculating $\mathbf{F}^*$. Note that $\mathbf{P}_n^*$ and $\mathbf{P}_t^*$ are the unknowns of our interest to be solved, not $\mathbf{P}_n$ and $\mathbf{P}_t$. It is therefore seen that the effect of the weighting function $W(\tau)$ may be covered by the introduction of β and γ only. It is also noted that the algorithm has a stability property identical to the Newark algorithm. The requirement for unconditional stability is known $2\beta \geqslant \gamma \geqslant \frac{1}{2}$.

COMPLEMENTARITY FORMULATION

The complementarity problem formulation derived in Kwak and Lee (1988) is adopted and extended to the dynamic case. By introducing slack variables $\mathbf{T}^+$ and $\mathbf{T}^-$, the Coulomb friction condition (30) can be rewritten as

$$\mathbf{P}_t + 2\mathbf{T}^- = \mu\mathbf{P}_n, \quad \mathbf{T}^- \geqslant 0, \tag{45}$$

$$-\mathbf{P}_t + 2\mathbf{T}^+ = \mu\mathbf{P}_n, \quad \mathbf{T}^+ \geqslant 0. \tag{46}$$

By integrating eqns (45) and (46) over the time interval with the weighting function W, we have

$$\mathbf{P}_t^* + 2\mathbf{T}^{-*} = \mu\mathbf{P}_n^*, \quad \mathbf{T}^{-*} \geqslant 0, \tag{47}$$

$$-\mathbf{P}_t^* + 2\mathbf{T}^{+*} = \mu\mathbf{P}_n^*, \quad \mathbf{T}^{+*} \geqslant 0, \tag{48}$$

where

$$\mathbf{T}^{-*} = \int_{-1}^{1} W\mathbf{T}^{-}\,\mathrm{d}\eta \Big/ \int_{-1}^{1} W\,\mathrm{d}\eta \quad \text{and} \quad \mathbf{T}^{+*} = \int_{-1}^{1} W\mathbf{T}^{+}\,\mathrm{d}\eta \Big/ \int_{-1}^{1} W\,\mathrm{d}\eta. \tag{49}$$

From eqns (47) and (48) the following relations are obtained:

$$\mathbf{T}^{+*}+\mathbf{T}^{-*} = \mu\mathbf{P}_n^*, \tag{50}$$

$$\mathbf{P}_t^* = \mathbf{T}^{+*}-\mathbf{T}^{-*}. \tag{51}$$

Now using eqns (41) and (51), the contact gap $\mathbf{D}_n^3$ and relative slip $\mathbf{D}_t^3$ at $\tau = \Delta t$ from eqns (25) and (26) can be represented in terms of $\mathbf{P}_n^*$, $\mathbf{T}^{+*}$, and $\mathbf{T}^{-*}$ as

$$\mathbf{D}_n^3 = \mathbf{D}_{nu}(\mathbf{U}^3-\mathbf{U}^1)+\mathbf{D}_{n0} = \mathbf{Q}_{11}\mathbf{P}_n^*+\mathbf{Q}_{12}\mathbf{T}^{+*}+\mathbf{Q}_{13}\mathbf{T}^{-*}+\bar{\mathbf{R}}_1, \tag{52}$$

$$\mathbf{D}_t^3 = \mathbf{D}_{tu}(\mathbf{U}^3-\mathbf{U}^1) = \mathbf{Q}_{21}\mathbf{P}_n^*+\mathbf{Q}_{22}\mathbf{T}^{+*}+\mathbf{Q}_{23}\mathbf{T}^{-*}+\bar{\mathbf{R}}_2, \tag{53}$$

where

$$\begin{aligned}
\mathbf{Q}_{11} &= \mathbf{D}_{nu}\mathbf{M}^{*-1}\mathbf{D}_{nu}^{\mathrm{T}},\\
\mathbf{Q}_{12} &= \mathbf{D}_{nu}\mathbf{M}^{*-1}\mathbf{D}_{tu}^{\mathrm{T}},\\
\mathbf{Q}_{13} &= -\mathbf{Q}_{12},\\
\mathbf{Q}_{14} &= (\Delta t)\mathbf{D}_{nu}\mathbf{M}^{*-1}(\mathbf{M}^*-\gamma\mathbf{K})\mathbf{M}^{-1}\mathbf{D}_{nu}^{\mathrm{T}},\\
\mathbf{Q}_{15} &= (\Delta t)\mathbf{D}_{nu}\mathbf{M}^{*-1}(\mathbf{M}^*-\gamma\mathbf{K})\mathbf{M}^{-1}\mathbf{D}_{tu}^{\mathrm{T}},\\
\mathbf{R}_1 &= \mathbf{D}_{nu}\mathbf{M}^{*-1}[-\mathbf{K}\mathbf{U}^1+\mathbf{F}^*+(\Delta t)(\mathbf{M}^*-\gamma\mathbf{K})\dot{\mathbf{U}}^1]+\mathbf{D}_{n0},\\
\mathbf{Q}_{21} &= \mathbf{Q}_{12}^{\mathrm{T}},\\
\mathbf{Q}_{22} &= \mathbf{D}_{tu}\mathbf{M}^{*-1}\mathbf{D}_{tu}^{\mathrm{T}},\\
\mathbf{Q}_{23} &= -\mathbf{Q}_{22},\\
\mathbf{Q}_{24} &= (\Delta t)\mathbf{D}_{tu}\mathbf{M}^{*-1}(\mathbf{M}^*-\gamma\mathbf{K})\mathbf{M}^{-1}\mathbf{D}_{nu}^{\mathrm{T}},\\
\mathbf{Q}_{25} &= (\Delta t)\mathbf{D}_{tu}\mathbf{M}^{*-1}(\mathbf{M}^*-\gamma\mathbf{K})\mathbf{M}^{-1}\mathbf{D}_{tu}^{\mathrm{T}},\\
\mathbf{R}_2 &= \mathbf{D}_{tu}\mathbf{M}^{*-1}[-\mathbf{K}\mathbf{U}^1+\mathbf{F}^*+(\Delta t)(\mathbf{M}^*-\gamma\mathbf{K})\dot{\mathbf{U}}^1],\\
\bar{\mathbf{R}}_1 &= \mathbf{Q}_{14}\Phi^0+\mathbf{Q}_{15}\Psi^0+\mathbf{R}_1,\\
\bar{\mathbf{R}}_2 &= \mathbf{Q}_{24}\Phi^0+\mathbf{Q}_{25}\Psi^0+\mathbf{R}_2.
\end{aligned} \tag{54}$$

The relative slip is expressed as a difference of two nonnegative values:

$$\mathbf{D}_t^3 = \mathbf{D}_t^{3+}-\mathbf{D}_t^{3-}, \quad \mathbf{D}_t^{3+} \geqslant 0, \quad \mathbf{D}_t^{3-} \geqslant 0. \tag{55}$$

Then the following complementarities hold:

$$\mathbf{D}_t^{3+\mathrm{T}}\mathbf{T}^{+*} = 0, \quad \mathbf{D}_t^{3+} \geqslant 0, \quad \mathbf{T}^{+*} \geqslant 0, \tag{56}$$

$$\mathbf{D}_t^{3-\mathrm{T}}\mathbf{T}^{-*} = 0, \quad \mathbf{D}_t^{3-} \geqslant 0, \quad \mathbf{T}^{-} \geqslant 0. \tag{57}$$

We also have a complementarity relation corresponding to contact condition (29):

$$\mathbf{D}_n^{3\mathrm{T}}\mathbf{P}_n^* = 0, \quad \mathbf{D}_n^3 \geqslant 0, \quad \mathbf{P}_n^* \geqslant 0. \tag{58}$$

Summarizing eqns (52), (53), (50), (58), (56) and (57), a linear complementarity problem is derived as

$$\mathbf{w} = \mathbf{D}\mathbf{z} + \mathbf{q}, \tag{59}$$

$$\mathbf{w}^{\mathrm{T}}\mathbf{z} = 0, \quad \mathbf{w} \geqslant 0, \quad \mathbf{z} \geqslant 0, \tag{60}$$

where

$$\begin{aligned}
\mathbf{w} &= \{\mathbf{D}_n^3, \quad \mathbf{D}_t^{3+}, \quad \mathbf{T}^{-*}\}^{\mathrm{T}}, \\
\mathbf{z} &= \{\mathbf{P}_n^*, \quad \mathbf{T}^{+*}, \quad \mathbf{D}_t^{3-}\}^{\mathrm{T}}, \\
\mathbf{D} &= \begin{bmatrix} \mathbf{Q}_{11} - \mu\mathbf{Q}_{12} & 2\mathbf{Q}_{12} & 0 \\ \mathbf{Q}_{12}^{\mathrm{T}} - \mu\mathbf{Q}_{22} & 2\mathbf{Q}_{22} & \mathbf{I} \\ \mu\mathbf{I} & -\mathbf{I} & 0 \end{bmatrix}, \\
\mathbf{q} &= \{\bar{\mathbf{R}}_1, \bar{\mathbf{R}}_2, 0\}^{\mathrm{T}}.
\end{aligned} \tag{61}$$

This linear complementarity problem (LCP), when solved by Lemke's algorithm (Bazaraa and Shetty, 1979), generates the state at $t = t_{n+1}$ or $\tau = \Delta t$.

IMPACT CONDITION

From the impact condition stated earlier we can consider the velocity discontinuities during impact. From eqns (25), (26) and (43), the normal and tangential components of the relative velocity at time $\tau = \Delta t$ can be represented as

$$\dot{\mathbf{D}}_n^3 = \mathbf{D}_{nu}\dot{\mathbf{U}}^3 = -\mathbf{D}_{nu}\mathbf{M}^{-1}\mathbf{D}_{nu}^{\mathrm{T}}\Phi^0 - \mathbf{D}_{nu}\mathbf{M}^{-1}\mathbf{D}_{tu}^{\mathrm{T}}\Psi^0 + \frac{2}{\Delta t}(\mathbf{D}_n^3 - \mathbf{D}_{n0}) - \dot{\mathbf{D}}_n^1, \tag{62}$$

$$\dot{\mathbf{D}}_t^3 = \mathbf{D}_{tu}\dot{\mathbf{U}}^3 = -\mathbf{D}_{tu}\mathbf{M}^{-1}\mathbf{D}_{tu}^{\mathrm{T}}\Phi^0 - \mathbf{D}_{tu}\mathbf{M}^{-1}\mathbf{D}_{tu}^{\mathrm{T}}\Psi^0 + \frac{2}{\Delta t}\mathbf{D}_t^3 - \dot{\mathbf{D}}_t^1, \tag{63}$$

where $\dot{\mathbf{D}}_n^1 = \mathbf{D}_{nu}\dot{\mathbf{U}}^1$ and $\dot{\mathbf{D}}_t^1 = \mathbf{D}_{tu}\dot{\mathbf{U}}^1$. Let us define

$$\begin{aligned}
J_I &= \{j: \quad P_{nj}^* > 0\}, \\
J_{st} &= \{j: \quad P_{nj}^* > 0 \quad \text{and} \quad D_{tj}^3 = 0\}, \\
J_{sl} &= \{j: \quad P_{nj}^* > 0 \quad \text{and} \quad |D_{tj}^3| > 0\},
\end{aligned} \tag{64}$$

where P_{nj}^* denotes the jth component of vector $\mathbf{P}_n^*$, J_{st} the set of sticking contact pairs, J_{sl} the set of slipping contact pairs and $J_I = J_{st} \cup J_{sl}$. When two bodies are in contact status, we have $D_{nj}^3 = \dot{D}_{nj}^3 = 0$ for $j \in J_I$. Then, from eqn (62),

$$\mathbf{D}_{nuj}\mathbf{M}^{-1}\mathbf{D}_{nuk}^{\mathrm{T}}\Phi_k^0 + \mathbf{D}_{nuj}\mathbf{M}^{-1}\mathbf{D}_{tuk}^{\mathrm{T}}\Psi_k^0 = -\dot{\mathbf{D}}_{nj}^1 - \frac{2}{\Delta t}\mathbf{D}_{n0j}, \quad j,k \in J_I, \tag{65}$$

where $\mathbf{D}_{nuj}$ and $\mathbf{D}_{tuj}$ denote the jth rows of $\mathbf{D}_{nu}$ and $\mathbf{D}_{tu}$, respectively. When a contact pair is in stick state, we have $D_{tj}^3 = \dot{\mathbf{D}}_{tj}^3 = 0$ for $j \in J_{st}$. Then, from eqn (63),

$$\mathbf{D}_{tuj}\mathbf{M}^{-1}\mathbf{D}_{nuk}^{\mathrm{T}}\Phi_k^0+\mathbf{D}_{tuj}\mathbf{M}^{-1}\mathbf{D}_{tuk}^{\mathrm{T}}\Psi_k^0=-\dot{\mathbf{D}}_{tj}^1,\quad j\in J_{st},\quad k\in J_l. \tag{66}$$

When a contact pair is in slip state, we can write as

$$\Psi_k^0=\mu\,\mathrm{sgn}(\mathbf{P}_{tk}^*)\Psi_k^0,\quad k\in J_{sl}, \tag{67}$$

where sgn(•) means the sign of (•). By solving eqns (65)–(67) solved for Φ^0 and Ψ^0, we can consider the velocity continuities as in the recurrence formula of eqns (41) and (43).

SOLUTION PROCEDURE

The solution procedure for the dynamic analysis of frictional contact problems can now be summarized as follows:

Step 0. Choose time integration parameters β and γ, and time interval Δt.
Step 1. Take $\Phi^0=\Psi^0=0$ and solve LCP (59) and (60) for $\mathbf{w}$ and $\mathbf{z}$ to get $\mathbf{D}_n^3$, $\mathbf{D}_t^3$, $\mathbf{P}_n^*$, and $\mathbf{P}_t^*$using eqns (51) and (55).
Step 2. Calculate Φ^0 and Ψ^0 from eqns (65)–(67) for each contact status. If $\Phi^0=\Psi^0=0$, then go to step 4. Otherwise go to step 3.
Step 3. Calculate $\bar{\mathbf{R}}_1$ and $\bar{\mathbf{R}}_2$ from eqn (54) and solve the LCP again to get $\mathbf{D}_n^3$, $\mathbf{D}_t^3$, $\mathbf{P}_n^*$, and $\mathbf{P}_t^*$.
Step 4. Calculate $\mathbf{U}^3$ and $\dot{\mathbf{U}}^3$ from eqns (41) and (43) and go to step 1 for the next time increment.

NUMERICAL EXAMPLES

Example 1. *Longitudinal impact of two elastic rods*

Two elastic rods with different lengths are subject to impact on their flat ends. Figure 2 shows the finite element mesh and a table of constants used. The same problem was solved by Asano (1981) and Jiang and Rogers (1988). The friction coefficient on the contact surface is assumed to be 0.1 and the plane stress condition is assumed. The time interval Δt for time integration is taken to allow the elastic wave to pass through at most one element of the smallest size during one step (Ta and Rogers, 1985). The wave velocity and the time interval are

$$c=\sqrt{\frac{E}{(1-\nu^2)\rho}}=5367.4\,\mathrm{m/s},$$

$$\Delta t=\frac{\Delta x}{c}=\frac{3.333\times10^{-3}}{5367.4}=0.621\times10^{-6}\,\mathrm{s}, \tag{68}$$

where c is the velocity of wave propagation, E the modulus of elasticity, ν Poisson's ratio, ρ the material density and Δx the length of the smallest element.

The results are compared with the one-dimensional theoretical solution without friction (Johnson, 1972) and those by ABAQUS, a commercial FE code (Hibbitt *et al.*, 1988). The normal contact stress at the rod center and edge of body 2 is shown in Fig. 3 with no numerical damping ($\gamma=0.5$, $\beta=0.25$). Though the numerical stress curve has some high frequency oscillations, the average value is very close to the theoretical one. Figure 4 shows the results with a small amount of numerical damping ($\gamma=0.6$, $\beta=0.3025$). Compared with the one-dimensional theoretical solution, the results show that the first release comes a little later and the second impact a little earlier. The results are very similar to those of Asano (1981) and Jiang and Rogers (1988). As to the results of ABAQUS, it shows larger oscillations than the present especially during the first impact. The present solution is also closer to zero than the ABAQUS during the first release. As Jiang and Rogers (1989)

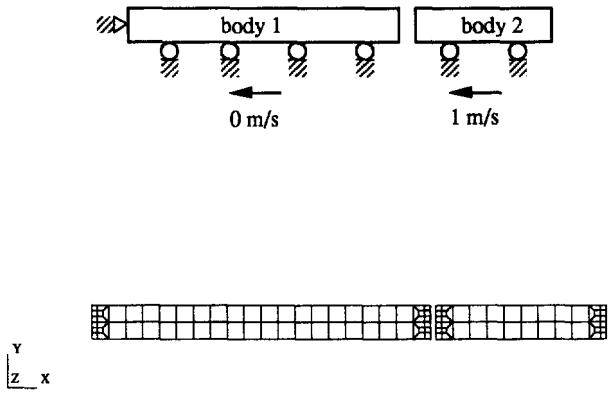

Data	Body 1	Body 2
Length (m)	0.2	0.1
Width (m)	0.02	0.02
Thickness (m)	0.001	0.001
Young's modulus (Pa)	2.508×10^{11}	2.508×10^{11}
Poisson's ratio	0.3	0.3
Density (kg/m^3)	0.785×10^{4}	0.785×10^{4}

Fig. 2. Finite element model for two-dimensional analysis for longitudinal impact of two rods.

Hughes (1987) and Holmes and Belytschko (1976) pointed out, the high frequency oscillations are caused by the finite element discretization of the continuum. Ko and Kwak (1992a, b) and Jian and Rogers (1989) have introduced proportional material damping to remove the oscillations.

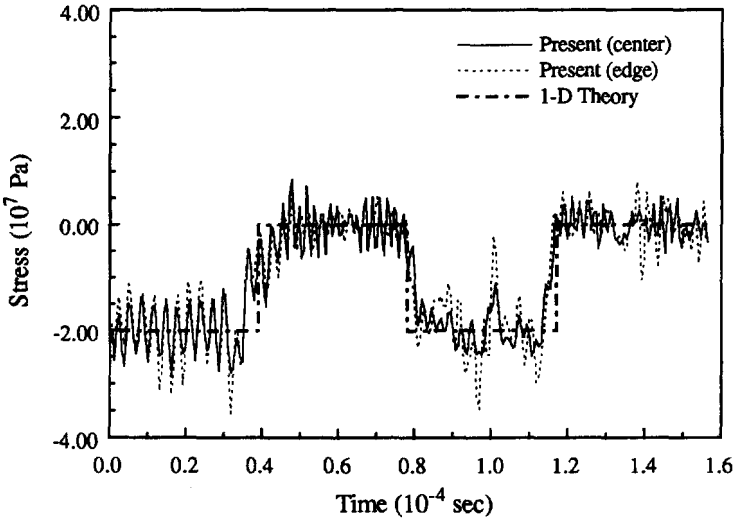

Fig. 3. Normal contact stress of body 2 ($\gamma = 0.5$, $\beta = 0.25$).

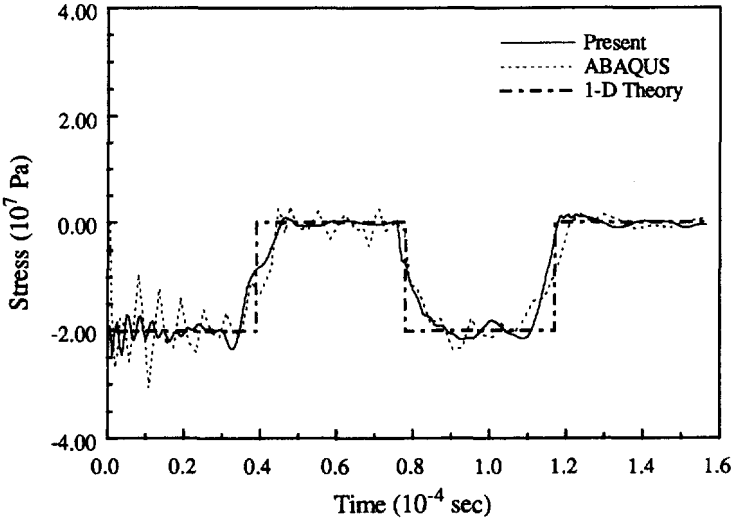

Fig. 4. Normal contact stress at rod center of body 2 ($\gamma = 0.6$, $\beta = 0.3025$).

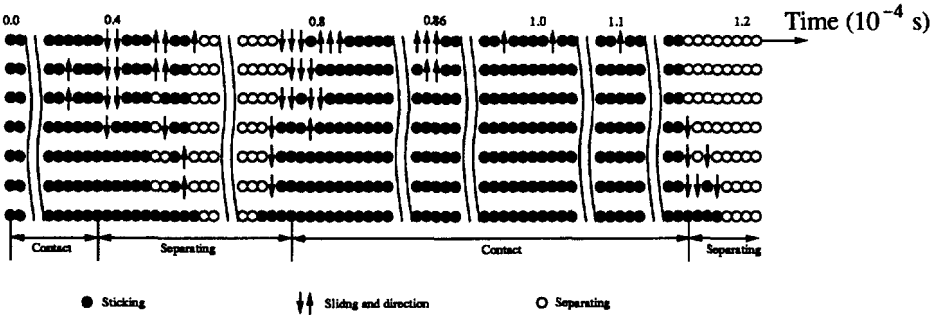

Fig. 5. Detailed behavior of contact nodes (no damping).

Figure 5 shows the sticking, slipping and separating contact status at the nodes on the contact surface of body 2. During contacting most of the contact pairs are in sticking status except near the first release, the second impact and the second release. This is similar to Asano (1981).

Example 2. *Oblique impact of a rectangular plate*

A rectangular plate is subject to oblique impact on a rigid wall as shown in Fig. 6. The plane stress condition is assumed and friction coefficients adopted are $\mu = 0.0$, 0.1 and 0.4. The time integration parameters chosen are $\gamma = 0.5$ and $\beta = 0.25$. The time interval Δt for time integration is taken as the time for the stress wave to pass through the smallest element as

$$c = \sqrt{\frac{E}{(1-\nu^2)\rho}} = 100\,\text{cm/s},$$

$$\Delta t = \frac{\Delta x}{c} = \frac{0.5}{100} = 0.005\,\text{s}. \tag{69}$$

Figures 7 and 8 display the variations of horizontal and vertical displacements at central point A of the moving plate as indicated in Fig. 6. The horizontal displacement is significantly influenced by the friction coefficient; the values of U_x become smaller as μ is larger. Moreover, the horizontal displacement U_x with $\mu = 0.0$ coincides with the rigid-body translation in the horizontal direction of the moving plate. Also, as seen in Fig. 8, the moving plate with higher friction coefficients shows larger rebounded vertical displacement U_y. It is noted that the central point A is separated, irrespective of the friction coefficient,

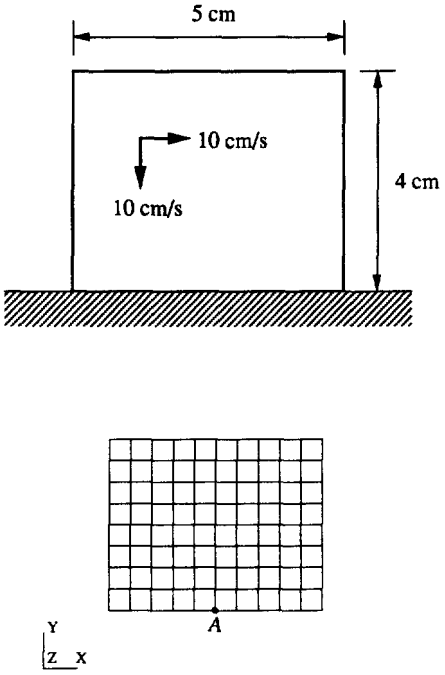

Thickness (cm)	1.0
Young's modulus (N/cm^2)	1.0
Poisson's ratio	0.0
Density (kg/cm^3)	0.01

Fig. 6. Finite element model for oblique impact of a rectangular plate.

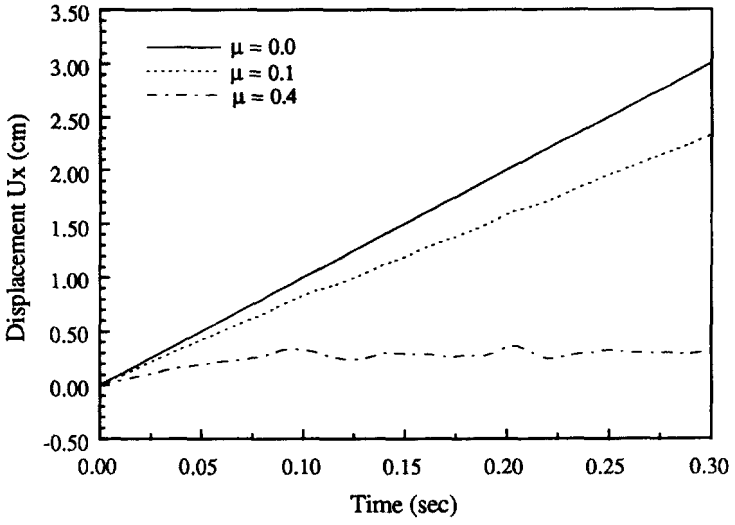

Fig. 7. Displacement U_x at point A ($\gamma = 0.5$, $\beta = 0.25$).

near time $t = 0.08$ s at which the reflecting elastic wave from the top surface arrives at the bottom surface of the plate.

The deformed shapes at time $t = 0.05$ s for various friction coefficients are shown in Fig. 9. The impacting body is more slanted with larger friction coefficient. Figure 10 shows the transient response of the plate with $\mu = 0.4$. After impact the plate is slanted to the

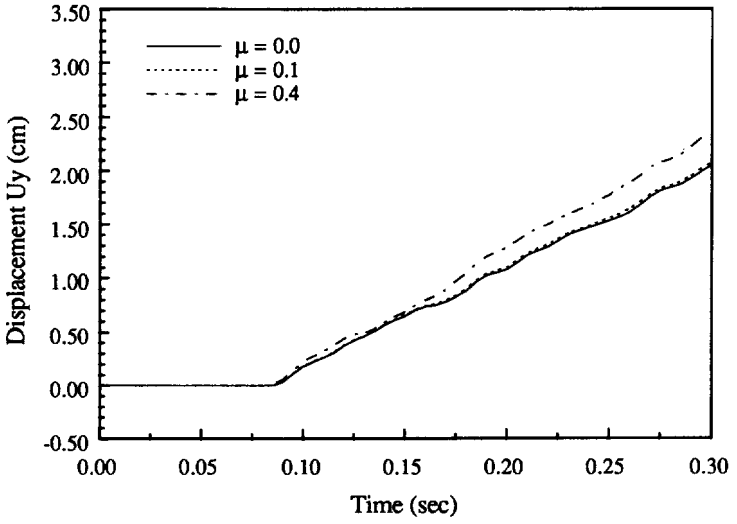

Fig. 8. Displacement U_y at point A ($\gamma = 0.5$, $\beta = 0.25$).

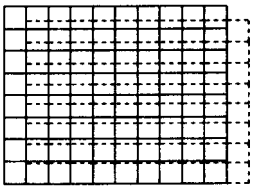

(a) $\mu = 0.0$

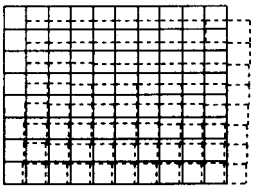

(b) $\mu = 0.1$

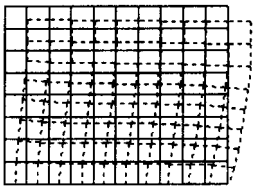

(c) $\mu = 0.4$

Fig. 9. Deformed shape at $t = 0.05$ s for various friction coefficients.

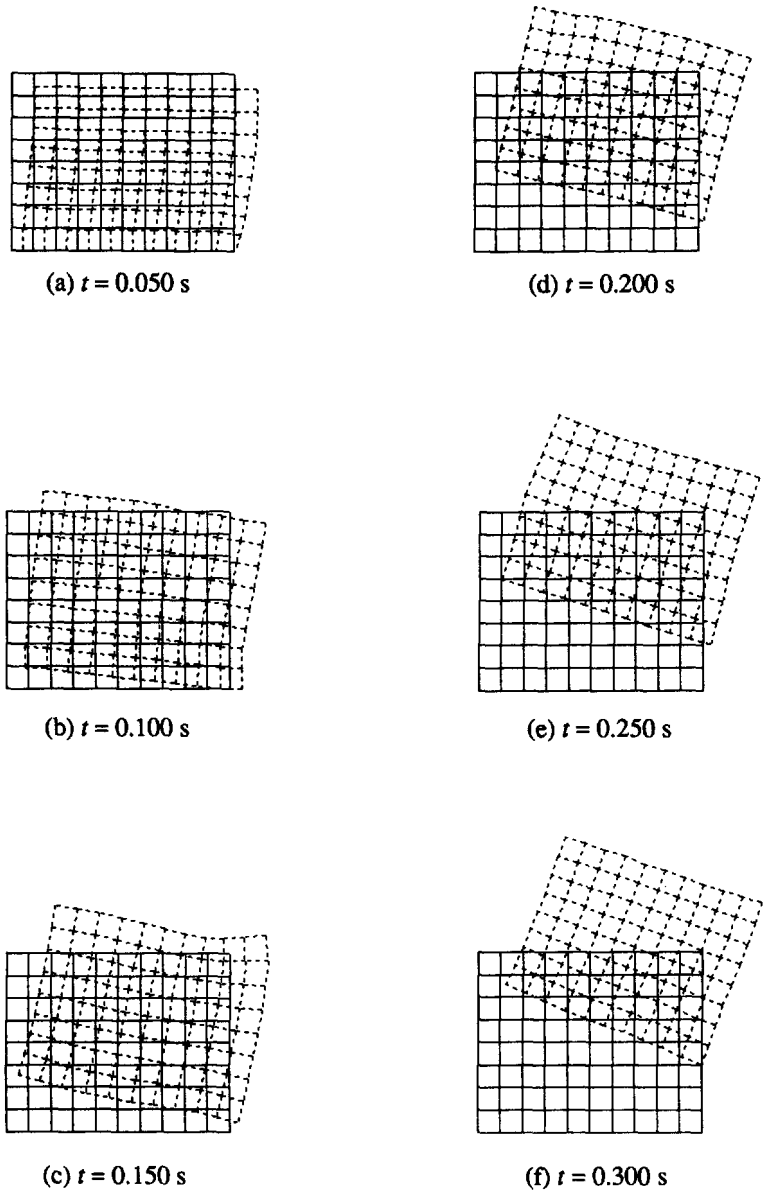

Fig. 10. Transient response vs time ($\mu = 0.4$).

right and the contact surface at the right is in stick while at the left in slip. The body also tends to rebound backwards (Maw *et al.*, 1981). The work done by the friction force in deflecting the body tangentially is stored as elastic strain energy and is recovered into kinetic energy after separation.

Example 3. *Oblique impact of a plate with a round boundary*

As shown in Fig. 11, a plate with a round end is subject to oblique impact on a rigid wall with initial velocity $V_x = 3$ m/s and $V_y = -5$ m/s. A similar problem was solved by Ko and Kwak (1992b) using triangular elements, while the present model uses 4-noded elements with more elements on contact surface. The plane stress condition is assumed and the friction coefficient used is $\mu = 0.1$. The time integration parameters are $\gamma = 0.5$, $\beta = 0.25$, and the time interval is $\Delta t = 1.0 \times 10^{-5}$ s, the same as Ko and Kwak (1992b).

Figures 12 and 13 show the contact normal and tangential forces, respectively. Contact occurs at node 5 first and then at nodes 6, 4, (7, 3), (8, 2) in turn. Release occurs at node 2 first and then at nodes 3, 8, 4, 7, 5, 6 in turn. Node 2 has the shortest contact duration. Compared with the normal forces, the tangential forces show somewhat different features

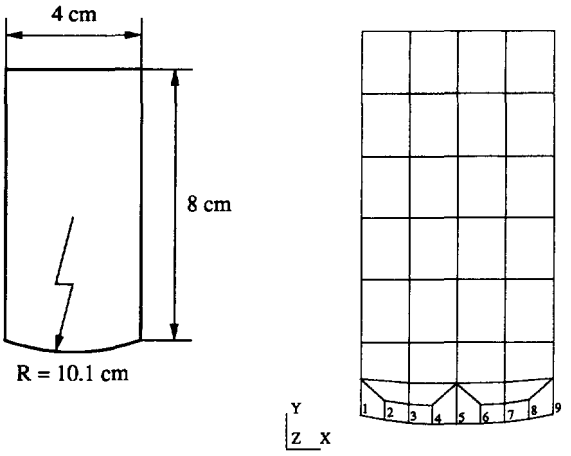

Thickness (m)	0.01
Young's modulus (Pa)	1.0×10^7
Poisson's ratio	0.25
Density (kg/m^3)	1.0×10^3

Fig. 11. Finite element model for oblique impact of a plate with a round boundary.

as in Fig. 13. The contact state is changed from stick to slip and vice versa at nodes 3 through 8. However, node 2 keeps slipping during contact and the contact force direction is not changed. At nodes 3, 4, 7, and 8, the friction force changes in direction for a few times while at node 5 it only does near the end of contacting. After a maximum tangential deformation of the body by the friction force is reached, the tangential force direction can be reversed. Compared with Ko and Kwak (1992b), the body is separated earlier.

As shown in Fig. 14, some of the kinetic energy is transformed into elastic energy during the compression stage and vice versa during restoration stage. Figure 15 shows a series of deformed shapes, which show the sequence of elastic deformation, translational displacement, and body rotation due to friction force.

For this oblique impact problem simulation, the computing time is about 430 s using a HP 720 workstation, which is much less than about 19,000 s of computation of Ko and Kwak (1992b) using a CRAY 2S super-computer. The proposed method for dynamic analysis of impact problem is very efficient.

CONCLUSION

A new method for the dynamic analysis of frictional contact is proposed. A linear complementarity problem formulation is derived from the compatibility condition of contact and the Coulomb friction condition. The discretized equation of motion is derived from Hamilton's law. For the time integration of dynamic response, displacements are approximated as second-order polynomials and an effective method of handling the velocity discontinuities during impact is presented. The time integration algorithm used has the same stability property as the Newmark method. From numerical examples, the efficiency of the proposed method is revealed.

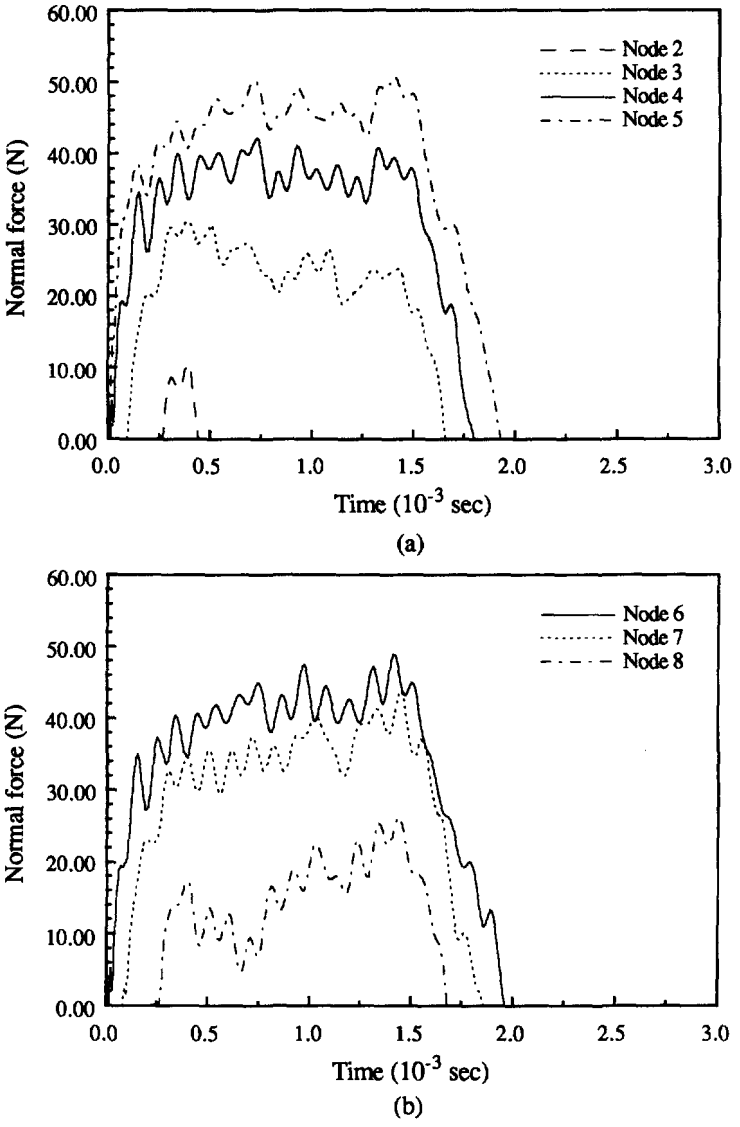

Fig. 12. Contact normal force ($\gamma = 0.5$, $\beta = 0.25$).

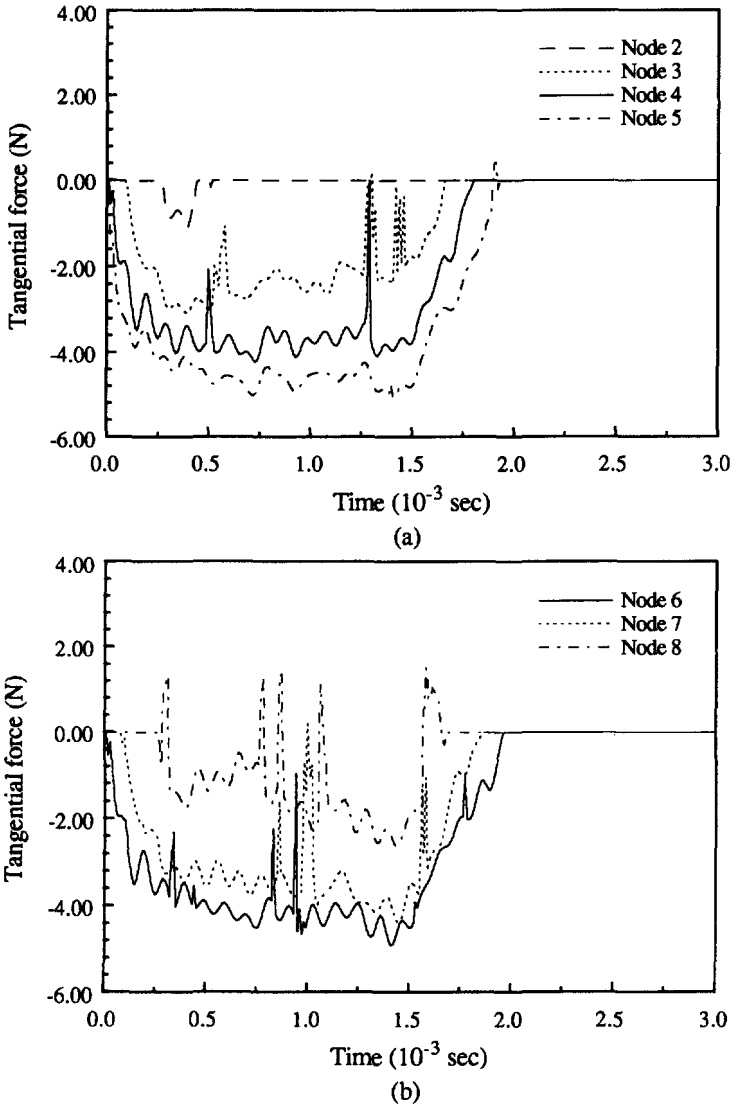

Fig. 13. Contact tangential force ($\gamma = 0.5$, $\beta = 0.25$).

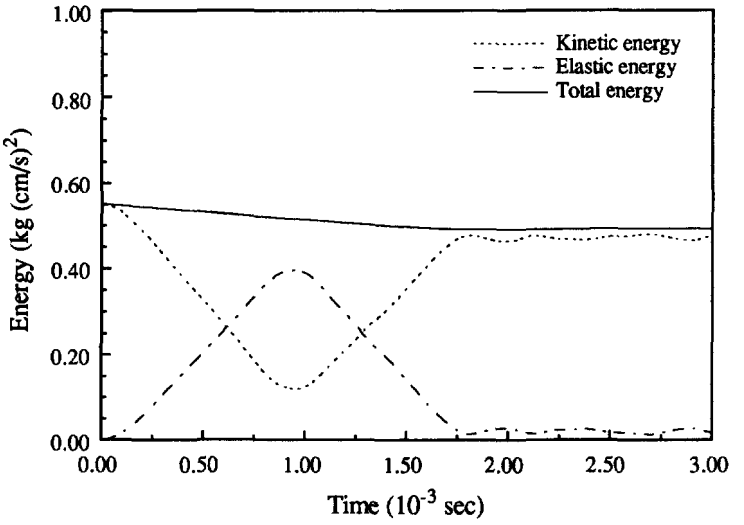

Fig. 14. Energy variation ($\mu = 0.1$, $\gamma = 0.5$, $\beta = 0.25$).

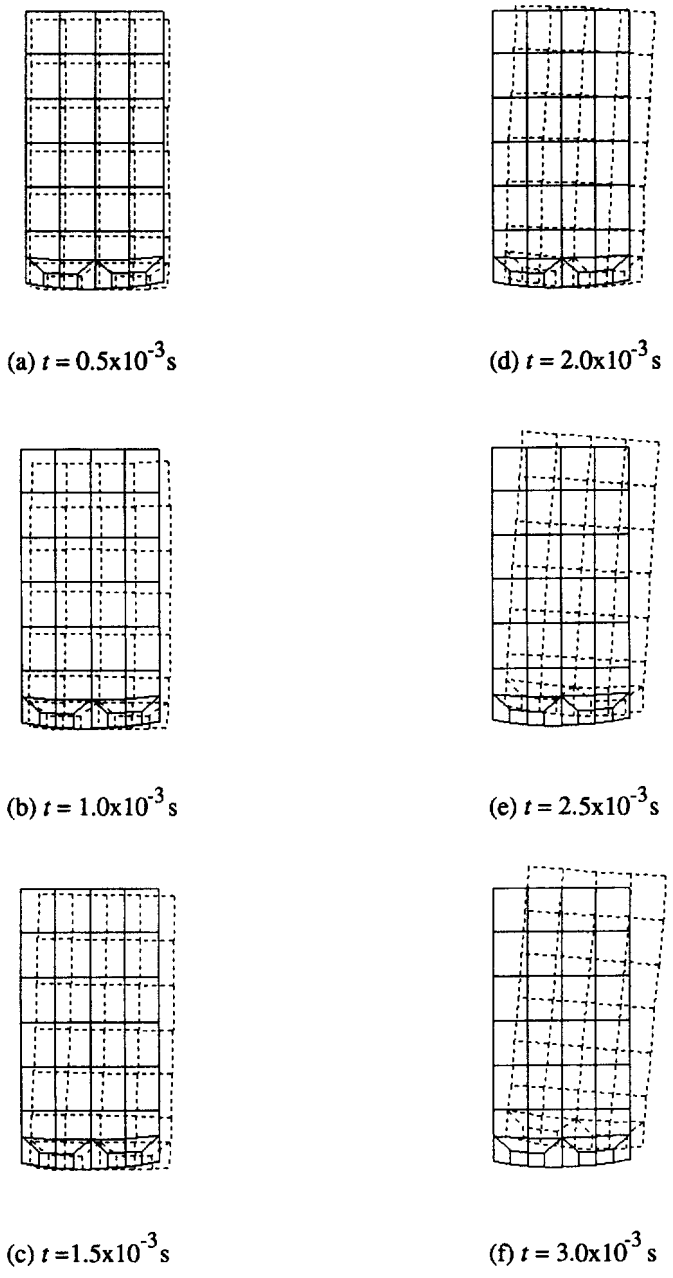

Fig. 15. Transient response vs time ($\mu = 0.1$).

REFERENCES

Asano, N. (1981). Principle of virtual work for two elasto-impact bodies in separate state and its applications to finite element method. *Bull. JSME* **24,** 1123–1129.

Bailey, C. D. (1975). Application of Hamilton's law of varying action. *AIAA J.* **13,** 1154–1157.

Bailey, C. D. (1980). The Galerkin formulation and the Hamilton–Ritz formulation: a comparison. *Acta Mech.* **36,** 63–70.

Bathe, K. J. (1982). *Finite Element Procedures in Engineering Analysis*, Prentice-Hall, New Jersey.

Bazaraa, M. S. and Shetty, C. M. (1979). *Nonlinear Programming: Theory and Algorithms*, John Wiley, New York.

Chen, W. H. and Tsai, P. (1986). Finite element analysis of elastodynamic sliding contact problems with friction. *Comput. Struct.* **22,** 925–938.

Hibbitt, Karlsson & Sorensen, Inc. (1988) *ABAQUS User's Manual.*

Holmes, N. and Belytschko, T. (1976). Postprocessing of finite element transient response calculations by digital filters. *Comput. Struct.* **6,** 211–216.

Hughes, T. J. R. (1987). *The Finite Element Method: Linear Static and Dynamic Finite Element Analysis*, Prentice-Hall, Singapore.

Hughes, T. J. R., Taylor, R. L., Sackman, J. L., Curnier A. and Kanoknukulchai, W. (1976). A finite element method for a class of contact-impact problems. *Comp. Meth. Appl. Mech. Engng* **8,** 249–276.

Huh, G. J. and Kwak, B. M. (1991). Constrained variational approach for dynamic analysis of elastic contact problems. *Finite Elem. Anal. Des.* **10,** 125–136.

Jiang, L. and Rogers, R. J. (1988). Combined Lagrangian multiplier and penalty function finite element technique for elastic impact analysis. *Comput. Struct.* **30,** 1219–1229.

Jiang, L. and Rogers, R. J. (1989). Proportional material damping in finite element impact analysis. *Comput. Struct.* **31,** 235–247.

Johnson, W. (1972). *Impact Strength of Materials*, Edward Arnold, London.

Kwak, B. M. (1991). Complementarity problem formulation of three-dimensional frictional contact. *ASME J. Appl. Mech.* **113,** 134–140.

Kwak, B. M. and Lee, S. S. (1988). A complementarity problem formulation for two-dimensional frictional contact problems. *Comput. Struct.* **28,** 469–480.

Ko, S. H. and Kwak, B. M. (1992a). Frictional dynamic contact analysis in deformable multibody systems. *Finite Elem. Anal. Des.* **12,** 27–40.

Ko, S. H. and Kwak, B. M. (1992b). Frictional dynamic contact analysis using finite element nodal displacement description. *Comput. Struct.* **42,** 797–807.

Maw, N., Barber, J. R. and Fawcett, J. N. (1991). The role of elastic tangential compliance in oblique impact. *ASME J. Lubr. Technol.* **103,** 74–80.

Ta, K. D. and Rogers, R. J. (1985). Control of elastic plane wave dispersion in two-dimensional finite element meshes. *Comput. Struct.* **21,** 1145–1151.

Talaslidis, D. and Panagiotopoulos, P. D. (1982). A linear finite element approach to the solution of the variational inequalities arising in contact problems of structural dynamics. *Int. J. Num. Meth. Engng* **18,** 1505–1520.

Zienkiewicz, O. C., Wood, W. L. and Hine, N. W. (1984). A unified set of single step algorithms part 1 : general formulation and applications. *Int. J. Num. Meth. Engng* **20,** 1529–1552.